

# Maximum Overheating and Partial Wetting of Nonmelting Solid Surfaces

Francesco D. Di Tolla, Furio Ercolessi, and Erio Tosatti

*International School for Advanced Studies (SISSA-ISAS), Via Beirut 4, I-34014 Trieste, Italy*

## Abstract

Surfaces which do not exhibit surface melting below the melting point (nonmelting surfaces) have been recently observed to sustain a very large amount of overheating. We present a theory which identifies a maximum overheating temperature, and relates it to other thermodynamical properties of the surface, in particular to geometrical properties more readily accessible to experiment. These are the angle of partial wetting, and the nonmelting-induced faceting angle. We also present molecular dynamics simulations of a liquid droplet deposited on Al(111), showing lack of spreading and partial wetting in good agreement with the theory.

PACS numbers: 68.10.Cr, 68.45.Gd, 61.50.Jr

For a long time crystal overheating above the bulk melting temperature  $T_m$  has been believed to be impossible, at least in the presence of a free clean surface. The standard argument [1,2] is that surface premelting will always take place and act as an ubiquitous seed for the liquid to grow. The well-known surface melting of Pb(110) [3,4] provided a first microscopic evidence of how liquid nucleation takes place on a solid below  $T_m$ . It was only a little later that simulations of Au(111) [5] and newer experiments on Pb(111) [6] and Al(111) [7] demonstrated microscopically that the opposite could also happen, namely that certain surfaces may exhibit nonmelting up to and in fact even *above* the melting point [5,8]. A solid bounded by such surfaces can therefore be *overheated*, although in a metastable state, above  $T_m$ . Métois *et al.* have first shown that small Pb particles with strictly (111) facets are easily overheated by a few degrees above  $T_m$  [9]. Even more strikingly, Herman *et al.* found that a flat nonmelting Pb surface can be overheated by as much as 120 K above  $T_m$  [10]. This implies that the free energy of a crystal surface can have a local minimum for zero liquid thickness. As in other nucleation problems one should thus expect the metastable overheated state to survive up to some instability temperature  $T_i > T_m$ , where the barrier finally disappears (fig. 1, inset). At present, however, there is no further available understanding of this phenomenon. In particular, there are no means to calculate  $T_i$  and possibly connect it with other quantities which are more readily measurable in a surface experiment. At a more microscopic level, it is very desirable to understand the different behavior of a nonmelting and of a melting surface, against nucleation of the liquid.

In this Letter, we introduce a simple theory of surface nonmelting which predicts the existence of a  $T_i$ , and connects its value with apparently unrelated geometrical quantities. These are the partial wetting angle  $\theta_m$  which a drop of melt will form with that crystal surface at  $T = T_m$ , and the faceting angle  $\theta_c$  of a vicinal surface. The angle  $\theta_m$  has also been rather commonly measured in the past, a few early examples being the (0001) face of Cd [11] and the (100) faces of several alkali halides [12]. The nonmelting-induced faceting [13,14] angle  $\theta_c$  has been well characterized experimentally and theoretically for (111) vicinals of Au [13,15], Cu [16] and Pb [13,14,17,18]. The connection we find between  $\theta_m$ ,  $\theta_c$  and

$T_i$  offers new insight in nonmelting surfaces. At a microscopic level, we substantiate this connection with molecular dynamics (MD) simulations of Al(111), which demonstrate both the non-spreading of a liquid drop at  $T_m$ , and the overheating of the flat face. The predicted relationship between  $\theta_m$ ,  $\theta_c$  and  $T_i$  is found to be in excellent agreement with the simulation results, as well as with experiments.

(i) *Theory*: Consider a liquid film of thickness  $\ell$ , sandwiched between semiinfinite solid and vapor, and let  $\ell$  grow from zero (no liquid) to a finite value. The change in free energy per unit area takes the standard form [4]

$$\Delta F(\ell) = \rho L \ell (1 - T/T_m) + \Delta\gamma(\ell) \quad (1)$$

where  $\rho$  is the liquid density,  $L$  the latent heat of melting, and  $\Delta\gamma(\ell)$  the difference between the overall free energy of the two interacting solid-liquid (SL) and liquid-vapor (LV) interfaces separated by a distance  $\ell$ , and the free energy of the solid-vapor (SV) interface. By definition,  $\Delta\gamma(0) = 0$ . Assuming short-range forces only, this term can phenomenologically be written as  $\Delta\gamma(\ell) = \Delta\gamma_\infty [1 - \exp(-\ell/\xi)]$  where  $\Delta\gamma_\infty \equiv \gamma_{\text{SL}} + \gamma_{\text{LV}} - \gamma_{\text{SV}}$  is the net free energy change upon conversion of the SV interface in two non-interacting SL and LV interfaces, and  $\xi$  is a correlation length in the liquid. For a melting surface  $\Delta\gamma_\infty < 0$ , and, for  $T_w < T < T_m$ ,  $\Delta F$  will have a minimum at  $\ell_0(T) = \xi \ln [T_m |\Delta\gamma_\infty| / (T_m - T) L \rho \xi]$  which is the mean-field thickness of the melted film [4]. The wetting temperature defined by  $\ell_0(T_w) = 0$  is  $T_w = T_m (1 - |\Delta\gamma_\infty| / L \rho \xi)$ .

For a *nonmelting surface*,  $\Delta\gamma_\infty > 0$ , and we move over to  $T > T_m$ . Here,  $\Delta F(\ell)$  will instead have a local minimum at  $\ell = 0$ , the absolute minimum for  $\ell \rightarrow \infty$ , and a *maximum* at a critical thickness

$$\ell_c(T) = \xi \ln \left[ \frac{T_m \Delta\gamma_\infty}{(T - T_m) L \rho \xi} \right] \quad (2)$$

as shown in fig. 1. The local minimum at  $\ell = 0$  signifies metastability of the crystalline surface for  $T < T_i$ , the maximum overheating temperature. The minimum disappears when  $\ell_c(T_i) = 0$ , yielding

$$T_i = T_m \left( 1 + \frac{\Delta\gamma_\infty}{L\rho\xi} \right). \quad (3)$$

Above  $T_i$ , the crystal surface will melt, no matter what its initial state is. In particular a surface which is initially crystalline will wet itself with a liquid film, which will grow, and gradually melt the whole crystal. Hence  $T_i$  can be seen as a non-equilibrium wetting temperature, or, more accurately, as a *spinodal* point for the overheated solid surface. For  $T_m < T < T_i$ , the predicted behavior is that typical of a nucleation problem. If the surface is prepared initially with a melted film of thickness  $\ell > \ell_c$  (upper vertical arrow in fig. 1), then melting will proceed, and  $\ell$  will grow to infinity, reaching full equilibrium. If, conversely, the starting thickness is less than  $\ell_c$ , then the surface will recrystallize, to reach the local, metastable minimum at  $\ell = 0$  (lower arrow in fig. 1). This peculiar behavior was first found and described in detail in an early simulation of the nonmelting surface Au(111) [5].

We now show that there is a simple connection between  $T_i$ , and the macroscopic non-wetting angle  $\theta_m$  at  $T = T_m$ . Following Nozières [19], the angles  $\theta_{LV}$ ,  $\theta_{SL}$ , formed by a drop of melt onto a nonwetting surface of the same material (fig. 2), satisfy the equations

$$\gamma_{SV} = \gamma_{LV} \cos \theta_{LV} + \gamma_{SL} \cos \theta_{SL} \quad (4)$$

$$R_{LV} \sin \theta_{LV} = R_{SL} \sin \theta_{SL} \quad (5)$$

where  $R_{LV}$ ,  $R_{SL}$  are the radii of respectively the LV and SL drop boundaries (supposedly spherical). Eq. (4) is simply the balance of lateral forces, while eq. (5) follows from simple geometry. Laplace's pressure equation  $P = 2\gamma/R$  determines the shape ratio  $x(T) \equiv R_{LV}/R_{SL} = \sin \theta_{SL}/\sin \theta_{LV} = [\gamma_{LV}P_{SL}(T)]/[\gamma_{SL}P_{LV}(T)]$ . Since  $P_{SL} \propto (T - T_m)$  near  $T_m$ , we expect  $\theta_{SL}$  to switch from negative for  $T < T_m$  to positive for  $T > T_m$ . At  $T = T_m$ ,  $x = \theta_{SL} = 0$ ,  $R_{LV} = \infty$ , and  $\theta_{LV} = \theta_m$  where

$$\cos \theta_m = 1 - \frac{\Delta\gamma_\infty}{\gamma_{LV}}. \quad (6)$$

Comparison of (6) with (3) shows that knowledge of  $\Delta\gamma_\infty$  at  $T = T_m$  determines *both*  $T_i$  and  $\theta_m$ , which are monotonically related by

$$\frac{T_i}{T_m} = 1 + \frac{2\gamma_{LV}}{L\rho\xi} \sin^2 \frac{\theta_m}{2}. \quad (7)$$

For a nonmelting surface there is a second important angle  $\theta_c$ , which is the nonmelting-induced faceting angle [13,14]. Consider vicinal faces tilted at an angle  $\theta$  away from the nonmelting face. At  $T = T_m$  there are two well-defined free energy minima (solid,  $\ell = 0$  and liquid,  $\ell = \infty$ ). We can thus draw [19] the two projected surface free energy branches  $\sigma(\theta) = \gamma(\theta)/\cos\theta$  as a function of the step density  $t = |\tan\theta|$ . The two branches are approximately given by the standard expressions

$$\sigma_S(\theta) = \gamma_{SV} + \mu t + g t^3 \quad (8)$$

$$\sigma_L(\theta) = (\gamma_{LV} + \gamma_{SL}) \sqrt{1 + t^2} \quad (9)$$

where  $\mu$  and  $g$  are the step free energy and the step-step repulsion on the solid surface. Here we have further assumed that  $\gamma_{SL}$  is approximately independent of  $\theta$ . The faceting angle is given by  $\theta_c = \arctan t_c$  which satisfies the double tangent construction:  $c_0 + c_1 t_0 = \gamma_{SV} + \mu t_0 + g t_0^3$ ,  $c_1 = \mu + 3g t_0^2$ , and  $c_0 + c_1 t_c = (\gamma_{LV} + \gamma_{SL}) \sqrt{1 + t_c^2}$ ,  $c_1 = (\gamma_{LV} + \gamma_{SL}) t_c / \sqrt{1 + t_c^2}$ . A particularly simple solution is obtained if the cubic (step-step repulsion) term  $g t_0^3$  can be ignored, whence  $t_0 = 0$ ,  $c_0 = \gamma_{SV}$ ,  $c_1 = [(\gamma_{LV} + \gamma_{SL})^2 - \gamma_{SV}^2]^{1/2}$  (note the nonanalyticity of  $\sigma_S$  at  $t = 0$ ) and  $t_c = \{[(\gamma_{LV} + \gamma_{SL})/\gamma_{SV}]^2 - 1\}^{1/2}$ . Even when this approximation cannot be made, and  $t_0$  is nonzero (as is the case for Pb(111) [14], where  $\arctan t_0 \simeq 2^\circ$ ), the above is still a pretty good approximation to the faceting angle, which is therefore simply related to  $\Delta\gamma_\infty$ :

$$\cos \theta_c \simeq \left(1 + \frac{\Delta\gamma_\infty}{\gamma_{SV}}\right)^{-1}. \quad (10)$$

Eq. (4) shows that  $\theta_c$  is identical to *both* the droplet angles  $\theta_{LV}$ ,  $\theta_{SL}$  at a single temperature  $T_u > T_m$ , satisfying  $x(T_u) = R_{LV}/R_{SL} = 1$ . We note that  $\theta_c$  is slightly smaller than  $\theta_m$ . The outer droplet angle  $\theta_{LV}$  will therefore decrease from  $\theta_m$  to  $\theta_c$  to zero when  $T$  is raised from  $T_m$  to  $T_u$  to  $T_i$ . Finally, we observe that a physical upper bound for  $\theta_m$  and  $\theta_c$  is given by

$\Delta\gamma_\infty \ll \gamma_{LV}$ , whence  $\theta_m \ll 90^\circ$ , and  $\theta_c \ll 60^\circ$ , i.e., a melt must at least partially wet its own solid.

(ii) *MD simulations:* Choosing Al(111) as our test case, we have simulated its behavior at and above  $T_m$  using the recent accurate glue potential of Ercolessi and Adams [20], derived by fitting to first-principles data. First, the approximate bulk melting point for this potential was determined using the phase coexistence technique [21] and found to be  $T_m = 939 \pm 5$  K (against an experimental value of  $T_m^{\text{exp}} = 933.6$  K). Then a 16-layers slab with 3 rigid bottom layers, one free surface, 224 atoms per layer and  $x$ - $y$  periodic boundary conditions, was studied as a function of  $T$ . As  $T_m$  was reached and crossed, the surface remained crystalline (metastable) as expected, up to a large  $T_i = 1088 \pm 18$  K =  $T_m + (149 \pm 18)$  K, even for very long (2 ns) runs. On the basis of our theory, using the known values of  $\rho = 0.0534 \text{ \AA}^{-3}$ ,  $L = 105.4 \text{ meV/atom}$  [20], and an estimated  $\xi = 2.6 \pm 0.3 \text{ \AA}$  [22], we extract from (3)  $\Delta\gamma_\infty = 2.3 \pm 0.4 \text{ meV \AA}^{-2}$ . Inserting in eq. (6), with an estimated value of  $\gamma_{LV} = 46.6 \text{ meV \AA}^{-2}$  (obtained with a separate simulation of the free liquid surface at  $T = T_m$ ) we finally predict  $\theta_m = (18 \pm 2)^\circ$  and, with a value  $\gamma_{SV} = 54.3 \text{ meV \AA}^{-2}$  [20],  $\theta_c = (16 \pm 2)^\circ$ .

To check this prediction, we have prepared an 861 Al-atom cluster which is fully melted and forms a liquid drop already at 900 K [23]. By depositing this Al drop on any given Al surface, we can learn about its wetting habit. We deposit it first on the Al(110) face, which is prone to melting [7]. At  $T = 930$  K (below  $T_m$ , but above  $T_w$ ), the drop spreads out completely within 100 ps (fig. 3a-c). However, when deposited on the nonmelting Al(111) face it does not diffuse away, but rather settles down as expected with well-defined exterior and interior angles whose azimuthal average  $\langle \theta \rangle$  we can extract. By increasing temperature across  $T_m$ , from 930 to 945 K, we find that  $\langle \theta_{LV} \rangle$  changes from  $(24 \pm 3)^\circ$  to  $(21 \pm 1)^\circ$ , and  $\langle \theta_{SV} \rangle$  from  $-\langle \theta_{LV} \rangle$  (the droplet is essentially crystallized) to  $(44 \pm 6)^\circ$ . By interpolation we extract  $\theta_m = (22 \pm 3)^\circ$ , in fairly good agreement with the predicted value  $(18 \pm 2)^\circ$ . The approximate values of  $\xi$ , and of  $\gamma_{LV}$  (about 20% lower than its experimental value, with our potential) constitute sources of error. Additional discrepancies are to be attributed to

the macroscopic and phenomenological nature of the theory, which should in principle be improved to include fluctuations and finite-size effects. On the simulation side, one could consider in the future finite-size scaling as a possibility.

(iii) *Connection with experiments:* We are not aware of measurements of  $\theta_m$ ,  $\theta_c$  or  $T_i$  on Al(111), for which we have thus a direct prediction. On Pb(111) van Pinxteren and Frenken [14] measured  $\theta_c = (14.7 \pm 1.4)^\circ$ , whence using eq. (10), and for  $\gamma_{SV} \simeq 34 \text{ meV}\text{\AA}^{-2}$  we obtain  $\Delta\gamma_\infty = 1.2 \pm 0.2 \text{ meV}\text{\AA}^{-2}$ . Furthermore, using  $\rho = 0.033 \text{\AA}^{-3}$ ,  $L = 50 \text{ meV/atom}$ , and  $\xi \simeq 2.7 \text{\AA}$  (averaging data from ref. [24] as suggested in [14]), we obtain via eq. (3)  $T_i = T_m + (150 \pm 30) \text{ K}$ . This is in rather good agreement with the experimental result,  $T_i^{\text{exp}} \simeq T_m^{\text{exp}} + 120 \text{ K}$  [10]. From eq. (6), using  $\gamma_{LV} \simeq 28 \text{ meV}\text{\AA}^{-2}$ , we also predict  $\theta_m = (16 \pm 1)^\circ$  for a droplet on Pb(111) at  $T = T_m$ . For Al(100), another nonmelting surface [25], we find by simulation  $T_i = 1025 \pm 5 \text{ K}$ , and assuming  $\xi \simeq 3 \text{\AA}$  we predict  $\theta_m \simeq 15^\circ$  and  $\theta_c \simeq 13^\circ$ . For Cd(0001), where  $\theta_m = (37 \pm 1)^\circ$  [11], and using  $\rho = 0.043 \text{\AA}^{-3}$ ,  $L = 64 \text{ meV/atom}$ ,  $\gamma_{LV} = 40 \text{ meV}\text{\AA}^{-2}$ , and again a guessed  $\xi \simeq 3 \text{\AA}$ , we get  $T_i \simeq T_m + 580 \text{ K}$ , close to twice the melting temperature (594 K). Application of this scheme to Ge(111) or NaCl(111) appears instead problematic, due to the essential role of long-range forces in these cases. In fact Ge(111) has a negative Hamaker constant, which is probably related to its nonmelting behavior [26], while long-range Coulomb forces are likely to be relevant to the nonmelting of NaCl(100). Finally, the present scheme is probably also inapplicable in its simplest form to surfaces such as Pb(100) or Au(100) which undergo *incomplete melting* [17,27–29].

In summary, we have described new results on the nonmelting crystal surfaces. A simple theory of nonmelting is given, which describes the metastable solid surface above  $T_m$ , up to a maximum overheating temperature  $T_i$  which acts as a spinodal point. This temperature is found to have a simple connection with the partial wetting angle of the surface by its own melt at  $T \approx T_m$ , and with the tilting angle of melted regions in vicinals undergoing nonmelting-induced faceting. Computer simulations on Al(111), as well as available data on Pb(111) are in good agreement with this theory.

We acknowledge instructive discussions with R. Evans, and support from EEC through

contracts ERBCHBGCT920180, ERBCHBGCT940636 and ERBCHRXCT930342, from INFN, and from CNR under project SUPALTTEMP.



## REFERENCES

- [1] J. Frenkel, *Kinetic theory of liquids* (Clarendon Press, Oxford, 1946), p. 425-6.
- [2] J. G. Dash, Contemp. Physics **30**, 89 (1989).
- [3] J. W. M. Frenken and J. F. van der Veen, Phys. Rev. Lett. **54**, 134 (1985).
- [4] J. F. van der Veen, B. Pluis, and A. W. Denier van der Gon, in *Chemistry and Physics of Solid Surfaces VII*, ed. by R. Vanselow and R. F. Howe (Springer, Heidelberg, 1988), p. 455.
- [5] P. Carnevali, F. Ercolessi, and E. Tosatti, Phys. Rev. B **36**, 6701 (1987).
- [6] B. Pluis *et al.*, Phys. Rev. Lett. **59**, 2678 (1987).
- [7] A. W. Denier van der Gon *et al.*, Surf. Sci. **227**, 143 (1990).
- [8] E. Tosatti, in *The Structure of Surfaces II*, ed. by J. F. van der Veen and M. A. Van Hove, (Springer, Berlin, 1988), p. 535.
- [9] J. J. Métois and J. C. Heyraud, J. Phys. (France) **50**, 3175 (1989).
- [10] J. W. Herman and H. E. Elsayed-Ali, Phys. Rev. Lett. **69**, 1228 (1992).
- [11] B. Mutaftschiev and J. Zell, Surf. Sci. **12**, 317 (1968).
- [12] G. Grange, and B. Mutaftschiev, Surf. Sci. **47**, 723 (1975); M. M. Dupuis, G. Grange, and B. Mutaftschiev, Phys. Stat. Sol. (a) **55**, 385 (1979); G. Grange, R. Landers, and B. Mutaftschiev, Surf. Sci. **54**, 445 (1976).
- [13] G. Bilalbegović, F. Ercolessi, and E. Tosatti, Surf. Sci. Lett. **258**, L676 (1991); Europhys. Lett. **17**, 333 (1992).
- [14] H. M. van Pinxteren and J. W. M. Frenken, Europhys. Lett. **21**, 43 (1993); H. M. van Pinxteren, B. Pluis, and J. W. M. Frenken, Phys. Rev. B **49**, 13798 (1994); H. M. van Pinxteren, Ph.D. thesis, Univ. of Amsterdam (1994).

- [15] K. D. Stock and B. Grosser, J. Cryst. Growth **50**, 485 (1980).
- [16] K. D. Stock, Surf. Sci. **91**, 655 (1980).
- [17] A. Pavlovskaja, K. Faulian, and E. Bauer, Surf. Sci. **221**, 233 (1989).
- [18] J. C. Heyraud, J. J. Métois, and J. M. Bermond, J. Cryst. Growth **98**, 355 (1989).
- [19] P. Nozières, J. Phys. (France) **50**, 2541 (1989).
- [20] F. Ercolessi and J. B. Adams, Europhys. Lett. **26**, 583 (1994).
- [21] F. Ercolessi, O. Tomagnini, S. Iarlori, and E. Tosatti, in *Nanosources and Manipulation of Atoms Under High Fields and Temperatures: Applications*, ed. by Vu Thien Binh, N. Garcia, and K. Dransfeld (Kluwer, Dordrecht, 1993), p. 185.
- [22] The interlayer distance is a lower bound for  $\xi$  ( $\xi \geq 2.3 \text{ \AA}$ ). Our assumed value is in agreement with estimates obtained with a new technique, based on the *collision* of the two interfaces (SL and LV) [O. Tomagnini *et al.*, unpublished (1994)].
- [23] See e.g. J.-P. Borel, Surf. Sci. **106**, 1 (1981); R. Kofman, P. Cheyssac, and R. Garrigos, Phase Transitions **24-26**, 283 (1990).
- [24] B. Pluis *et al.*, Surf. Sci. **239**, 265 (1990).
- [25] A. M. Molenbroek and J. W. Frenken, Phys. Rev. B **50**, 11132 (1994)
- [26] N. Takeuchi, A. Selloni, and E. Tosatti, Phys. Rev. Lett. **72**, 2227 (1994).
- [27] H. M. van Pinxteren and J. W. M. Frenken, Surf. Sci. **275**, 383 (1992).
- [28] B. M. Ocko *et al.*, Phys. Rev. B **44**, 6429 (1991), and references therein.
- [29] G. Bilalbegović and E. Tosatti, Phys. Rev. B **48**, 11240 (1993)

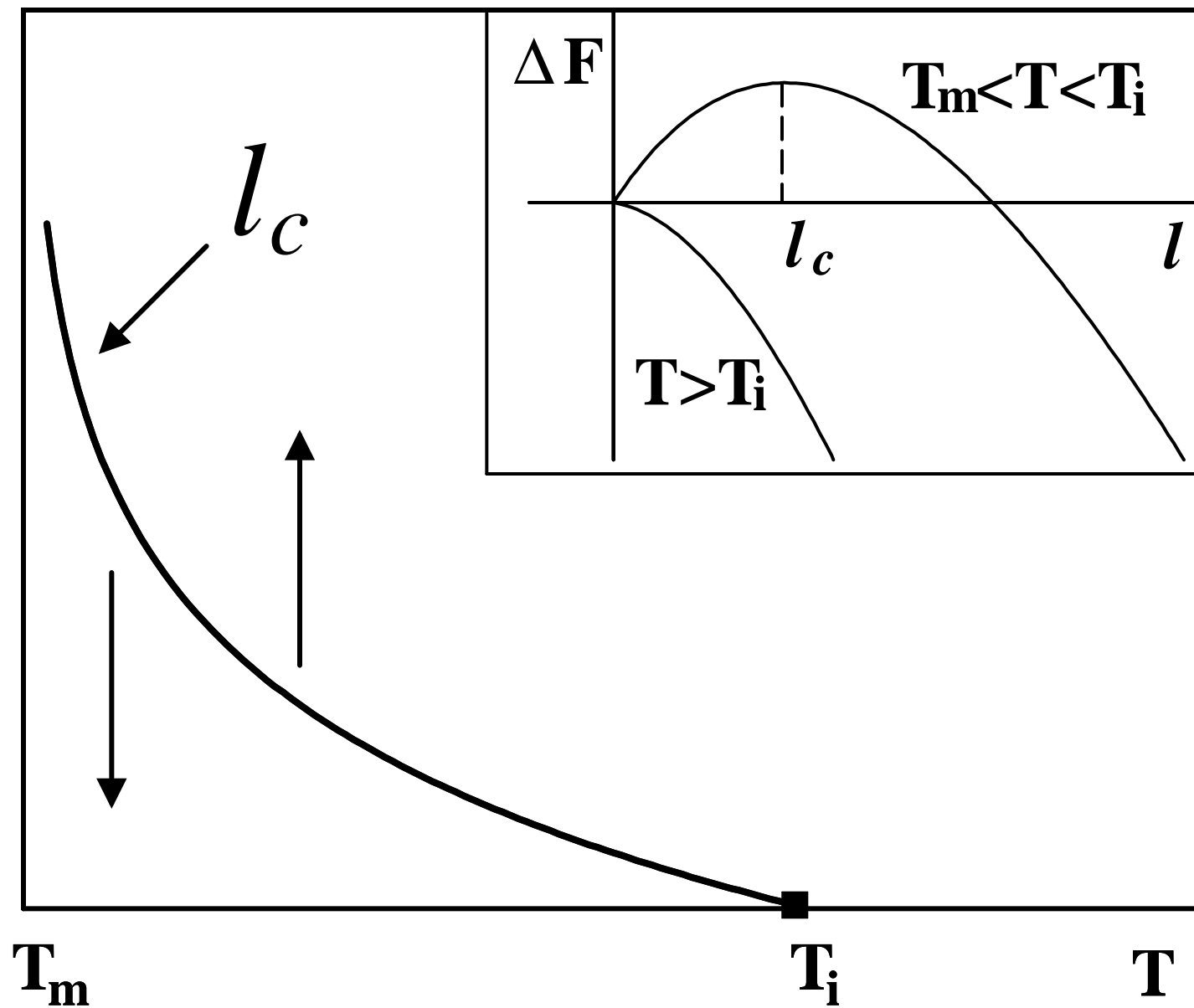
## FIGURES

FIG. 1. Critical liquid thickness of a nonmelting surface vs. temperature above  $T_m$  (schematic). A system with a liquid film thinner than the critical value, will recrystallize for any  $T$  between  $T_m$  and  $T_i$ . One with a thicker film will melt completely. Inset: free energy change upon conversion of a film of thickness  $\ell$  from solid to liquid. From  $T_m$  to  $T_i$  the solid surface is a local minimum.

FIG. 2. Shape of a drop of melt onto a nonmelting solid surface of the same material. The two interfaces separating solid and liquid (SL), and liquid and vapor (LV) are assumed to be spherical, with radii  $R_{SL}$  and  $R_{LV}$  and contact angles  $\theta_{SL}$  and  $\theta_{LV}$  respectively.

FIG. 3. Evolution of an 861-particles liquid drop of Al on substrate of the same material. Left column: drop on a surface undergoing surface melting (Al(110) at  $T = 0.99 T_m$ ). (a) before contact; (b) after contact, the drop spreads readily; (c) the drop has been fully absorbed. Right column: drop on a nonmelting overheated surface (Al(111) at  $T = 1.01 T_m$ ). (d) before contact; (e) after contact: the drop settles, but does not spread; (f) final drop shape. Darkness of atoms is proportional to their square displacement in the run.

LIQUID FILM THICKNESS



**vapor**

**$R_{SL}$**

**$\theta_{LV}$**

**$\theta_{SL}$**

**liquid**

**$R_{LV}$**

**solid**

